DESIGN AND MEASURED BEHAVIOR OF A PERFORATED HYBRID PRECAST CONCRETE SHEAR WALL FOR SEISMIC REGIONS

Brian J. Smith, PE, Dept. of Civil Eng. and Geo. Sci., Univ. of Notre Dame, USA
Yahya C. Kurama, PhD, PE, Dept. of Civil Eng. and Geo. Sci., Univ. of Notre Dame, USA
Michael J. McGinnis, PhD, Dept. of Civil Engineering, University of Texas at Tyler, USA

ABSTRACT

This paper focuses on the design and measured behavior of a 0.4-scale perforated "hybrid" precast concrete shear wall for use in seismic regions. The wall structure that is investigated utilizes a combination of mild (i.e., Grade 60) steel and high-strength unbonded post-tensioning (PT) steel for lateral resistance across horizontal joints. The mild steel reinforcement is designed to yield in tension and compression, providing energy dissipation. The unbonded PT steel provides self-centering capability, reducing the residual lateral displacements of the wall after a large earthquake. Both the PT steel and the mild steel contribute to the lateral strength, resulting in an efficient structure. A unique feature of the test specimen is the inclusion of rectangular perforations inside the wall panels. The paper discusses a seismic design approach that utilizes a finite-element model subjected to a monotonic lateral load analysis to design the bonded reinforcement around the panel perforations. The analytical model intentionally incorporates several simplifying assumptions appropriate for the design office. The results from a pre-test analytical study are compared with experimental measurements of the wall specimen subjected to reversed-cyclic lateral loading, focusing on the global response of the structure. Ultimately, these analytical and experimental results are expected to support the successful validation and code approval of hybrid precast concrete shear walls for moderate and high seismic regions of the U.S.

Keywords: Horizontal Joints, Hybrid Shear Walls, Perforated Shear Walls, Precast Concrete, Seismic Testing, Wall Opening Design

INTRODUCTION AND BACKGROUND

Concrete shear walls make up a large percentage of the primary lateral load resisting systems in U.S. building construction. As shown in Figure 1, the hybrid precast concrete shear wall configuration investigated in this research is constructed by placing rectangular wall panels across horizontal joints. This system is a type of "non-emulative" precast structure where the wall behavior under lateral loads is different than the behavior of an otherwise comparable monolithic cast-in-place reinforced concrete system.
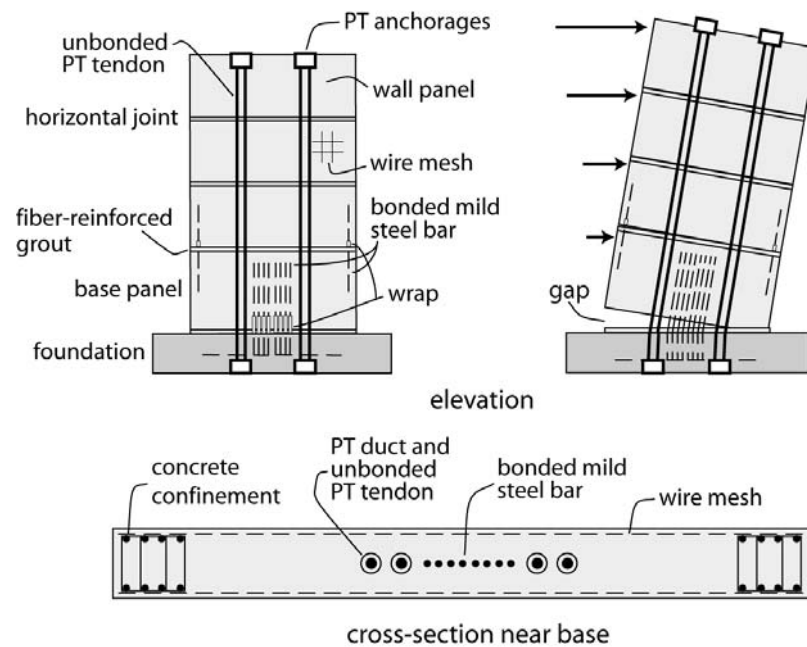

Fig. 1   Elevation, Exaggerated Displaced Position, and Cross-Section of Hybrid Wall System

Under the application of lateral loads into the nonlinear range, the primary mode of displacement in hybrid walls occurs through gap opening at the horizontal joint between the base panel and the foundation, allowing the wall to undergo large lateral displacements with little damage. A combination of mild (i.e., Grade 60) steel and high-strength unbonded post-tensioning (PT) steel is used for lateral resistance across these joints, resulting in an efficient structure. Upon unloading, the PT steel provides a restoring force to close this gap, thus reducing the residual (i.e., permanent) lateral displacements of the wall after a large earthquake. The use of unbonded tendons delays the yielding of the PT strands and reduces the tensile stresses transferred to the concrete (thus reducing cracking) as the tendons elongate under lateral loading. Mild steel bars are designed across the base joint to yield in tension and compression, and provide energy dissipation through the gap opening/closing behavior of the wall. A pre-determined length of these energy dissipating bars is unbonded at the bottom of the base panel (by wrapping the bars with plastic sleeves) to reduce the steel strains and prevent low-cycle fatigue fracture.

The hybrid precast wall system offers high quality production, relatively simple construction, and excellent seismic characteristics by providing self-centering to the building (i.e., the wall returns to its undisplaced "plumb" position after a large earthquake) as well as sufficient energy dissipation to control the lateral displacements. Despite these desirable characteristics,

there are significant limitations that prevent the use of hybrid walls in seismic regions of the U.S. Most importantly, Chapter 21 of ACI 318[1] specifies that "a reinforced concrete structural system not satisfying the requirements of this chapter shall be permitted if it is demonstrated by experimental evidence and analysis that the proposed system will have strength and toughness equal to or exceeding those provided by a comparable monolithic reinforced concrete structure satisfying this chapter." Since the new wall system falls within this "non-emulative" category, experimental validation is required prior to its use in practice. In accordance with this requirement, this paper discusses the design and measured behavior of a recently-tested hybrid shear wall specimen featuring multiple rectangular perforations inside the precast wall panels.

OBJECTIVES AND SCOPE

The most pressing U.S. market need related to hybrid precast walls is code approval for use in moderate and high seismic regions per ACI 318. Achieving this task would lift a major road block and advance building construction. To address the current market need, the primary objective of this project is to support the validation of hybrid wall structures as "special" reinforced concrete shear walls through an integrated experimental and analytical study. The minimum experimental evidence needed to achieve this objective is specified by ACI ITG-5.1.[2] Among the subjects covered in ACI ITG-5.1 are requirements for the design of the test specimens and their configurations, as well as requirements for testing, assessing, and reporting satisfactory performance. Design guidelines and requirements for special unbonded post-tensioned precast shear walls satisfying ACI ITG-5.1 can be found in ACI ITG-5.2.[3]

To date, limited tests and analytical studies are available for hybrid precast walls (Smith et al;[4] Rahman and Restrepo;[5] Holden et al;[6] Kurama[7,8]). While these results have demonstrated the excellent behavior that can be obtained from these structures, concrete shear walls often feature perforations to allow for windows and doors to be incorporated into the building system. Previous research on precast concrete walls featuring perforations inside the panels is extremely limited (Allen and Kurama;[9] Mackertich and Aswad[10]), and there are currently no results published on hybrid walls with perforations. This paper focuses on this important knowledge gap.

TEST SET-UP AND SPECIMEN PROPERTIES

A photograph of the test specimen described in this paper and a schematic of the test setup are shown in Figure 2. The wall specimen was designed for a 4-story prototype parking garage structure in Los Angeles, CA, with an approximate building footprint of 42,000 sq-ft. More details on this prototype structure are provided in Smith et al.[4] The test was conducted at 0.4-scale, which satisfies the minimum scaling limit of ACI ITG-5.1. Another requirement of ACI ITG-5.1 is that the specimen be constructed using a minimum of two wall panels

since the prototype structure uses a separate panel for each story. In accordance with this requirement, the test wall featured two panels: the lower panel representing the base panel and the upper panel representing the 2nd through 4th stories of the prototype wall. It was possible to model the upper story panels of the prototype wall using a single panel since no gap opening was expected at the joints between these panels. The wall length, l_w, was 96 in. and the wall height to length aspect ratio was h_w/l_w=2.25. The height of the base panel, h_{pb}, was 57 in. and the panel thickness, t_p, was 6.25 in. Each wall panel featured two rectangular perforations, each with length, l_o=14 in. and height, h_o=20 in. The perforations were placed in a symmetrical layout with respect to the wall centerline, with the exterior edges of the perforations located 14 in. from the panel edge and 14 in. from the panel base. The perforations in the upper panel represented those in the 2nd story. The perforations in the 3rd and 4th stories of the prototype wall were not modeled since they would be less critical than the lower story perforations.

(Front Face of Wall) NORTH →

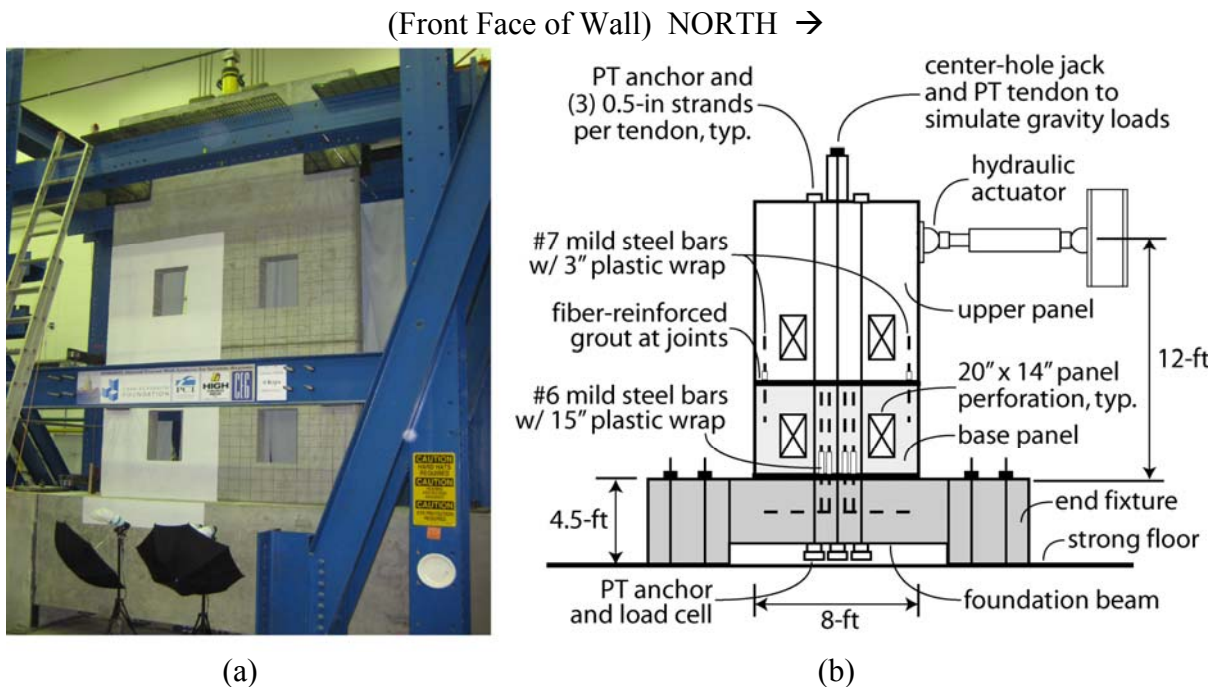(a)   (b)

Fig. 2 Test Set-Up: (a) Photograph; (b) Schematic Drawing

The PT steel consisted of two bundles of strand located 11 in. north and south from the wall centerline. Each PT bundle included three 0.5 in. diameter strands (design ultimate strength=270 ksi) with an unbonded length from the top of the wall to the bottom of the foundation beam of 18.25 ft. The mild steel reinforcement crossing the base joint consisted of four #6 bars (measured yield strength=65.5 ksi), with one pair of bars located 3.5 in. north and south from the wall centerline and the other pair 7.5 in. north and south from the centerline. These energy dissipating bars were unbonded over a length of 15 in. at the bottom of the base panel. Across the upper panel-to-panel joint, two #7 bars were used, with one bar located 4 in. from each end of the wall. This reinforcement was designed not to yield so as to

limit any gap opening along the panel-to-panel joint. To prevent strain concentrations, a short 3 in. length of these bars was unbonded at the bottom of the upper panel. The lateral load was applied at the resultant location of the 1st mode inertial forces (12 ft. from the wall base), resulting in a wall base moment to shear ratio of $M_b/V_b=1.5l_w$.

FINITE-ELEMENT ANALYTICAL MODEL

As required by ACI ITG-5.1, a pre-test study was conducted to evaluate the design of the test specimen based on nonlinear lateral load analyses. A detailed design procedure and analytical models for solid hybrid walls can be found in Smith et al.[4] and Smith and Kurama.[11] The design procedure for perforated walls closely follows this procedure, with an additional step to design the bonded horizontal and vertical reinforcement around the perforations as well as the shear reinforcement in each horizontal and vertical chord member. For this purpose, a finite-element model of the specimen was developed using the ABAQUS Program (Hibbitt et al.[12]) and a monotonic pushover analysis of the wall was conducted. This model is more detailed than the finite-element model presented in Smith et al.[4] for solid walls, as several of the simplifications have been eliminated (such as lumping the PT and energy dissipating steel areas at the wall centerline, excluding the contact surface at the upper panel-to-panel joint, and excluding the mild steel crossing the upper panel-to-panel joint). However, the modeling philosophy was kept consistent and intended to create a basic analysis tool that intentionally incorporated simplifying assumptions appropriate for the design office.

As shown in Figure 3, the perforated hybrid wall model included three-dimensional eight-node stress/displacement solid elements for the wall panels and the foundation fixtures. Three-dimensional stress/displacement truss elements were used for the PT steel, energy dissipating mild steel crossing the base joint, and mild steel reinforcement crossing the upper joint. To allow for gap opening at the horizontal joints, the model incorporated "hard" contact surfaces at these joints.

Fig. 3   Finite-Element (ABAQUS) Modeling of Perforated Hybrid Wall Test Specimen
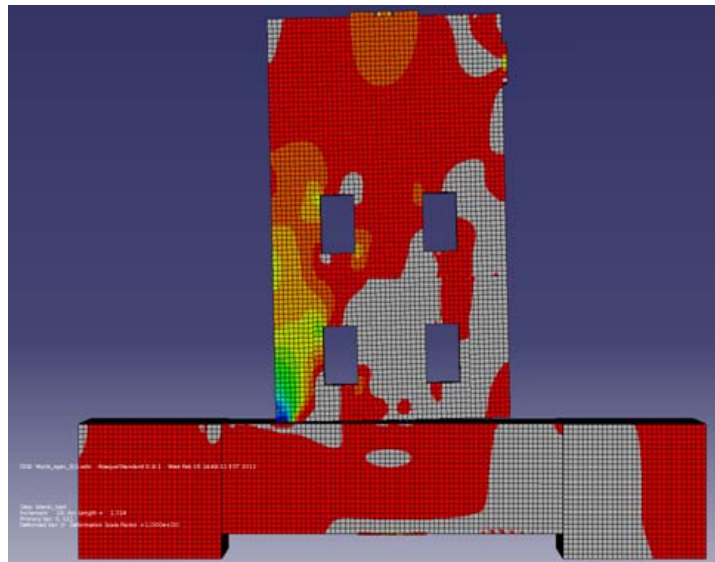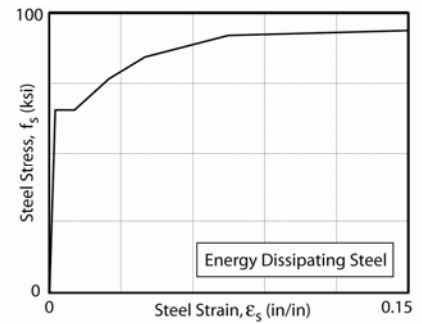
The stress-strain relationships for the PT steel and energy dissipating mild steel bars were modeled using a multiple-point approximation of the measured monotonic material test data, as shown in Figure 4. Each material model included "elastic"

and "plastic" regions as defined in ABAQUS. To represent the end anchorages of the PT tendons, steel anchorage plates were modeled and connected to the foundation and upper panel concrete elements using "tie
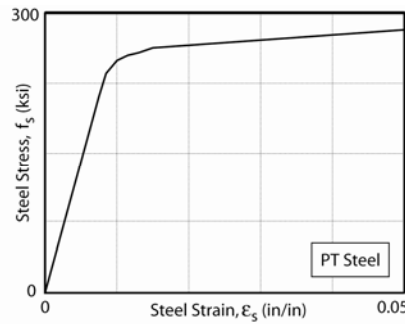
(a)

(b)

Fig. 4   Steel Stress-Strain Relationships: (a) PT Steel; (b) Energy Dissipating Mild Steel

constraints." The truss elements modeling the anchored ends of the PT tendons were then embedded within these anchorage plate elements using "embedded region constraints." The initial post-tensioning stresses in the PT steel were simulated by placing an initial tension force in the truss elements for the tendons.

The truss elements modeling the energy dissipating mild steel bars across the base joint were partitioned into bonded and unbonded regions. In the bonded regions of the bars (located in both the base panel and the foundation), the truss elements were embedded within the concrete elements using embedded region constraints. The elements in the unbonded regions were not constrained, thereby allowing a uniform strain distribution to form over the unbonded length. The bonded and unbonded portions of the mild steel reinforcement across the upper joint were modeled in the same manner.

As shown in Figure 5, the concrete behavior in compression was also modeled using a multiple-point approximation of the material stress-strain relationships (with "elastic" and "plastic" regions). The unconfined concrete stress-strain behavior was created based on the measured concrete strength and initial stiffness using the relationship from Popovics.[13] For confined concrete, the confinement reinforcement was not modeled explicitly in the finite-element analysis, but was represented through a uniaxial confined concrete stress-strain relationship created using Mander et al.[14] Any additional concrete confinement effects developing due to the transverse stresses in the finite-element model were ignored.
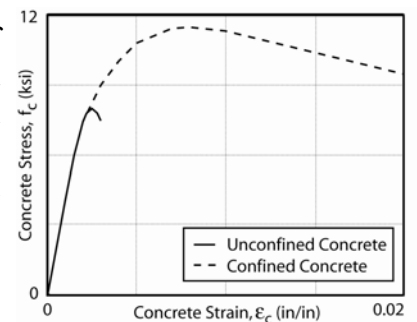

Fig. 5   Concrete Stress-Strain Relationships in Compression

To achieve a reasonably simple model suitable for design practice, the bonded mild steel reinforcement contained within the wall panels and the foundation beam (except for the continuous steel across the horizontal joints) was not modeled explicitly. Instead, the effect of the bonded steel reinforcement inside each wall component was captured using elastic

tension properties for the concrete. It was assumed that the wall panels and the foundation beam contained a sufficient amount of bonded mild steel reinforcement to limit the size of the cracks, and that this reinforcement did not yield. Based on these assumptions, the required area of the bonded reinforcement inside the panels was determined from the tension stresses developing in the concrete as explained in more detail below. Note that as a result of using elastic tension properties for the concrete, the redistribution of stresses due to cracking was not modeled. However, in a properly designed wall with sufficient and well-distributed reinforcement, the concrete cracks remain small and are not expected to significantly affect the overall behavior. The biggest "crack" in a hybrid precast concrete wall is the gap that forms at the base joint, which is appropriately included in the model by using contact surfaces at this joint

DESIGN OF BONDED REINFORCEMENT AROUND PERFORATIONS

The finite-element model of the test specimen was subjected to a monotonic pushover analysis through the prescribed validation-level drift of Δ_w=+2.30% (determined based on the requirements of ACI ITG-5.1) and up to a maximum drift of Δ_w=3.05%. As previously mentioned, the resulting concrete tension stresses from this analysis were used to design the bonded horizontal and vertical reinforcement around the panel perforations as well as the shear reinforcement in each horizontal and vertical chord member (see Figure 6).
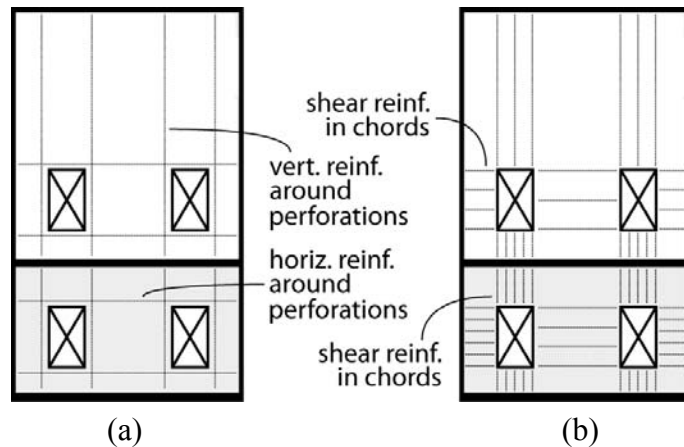

Fig. 6 Additional Bonded Panel Reinforcement due to Presence of Perforations: (a) Horizontal and Vertical Reinforcement; (b) Shear Reinforcement

The finite-element stresses at the validation-level drift were used in the design. Figure 7 shows the x-direction (i.e., horizontal) stresses, y-direction (i.e., vertical) stresses, and shear stresses obtained from the model. For clarity, only the critical regions of the wall with tensile stresses are displayed in color, with the regions in compression colored in black. As shown in Figures 7a and 7b for the x and y-directions, respectively, the bonded horizontal and vertical reinforcement around the perforations was designed by summing the tensile stresses along a cutline (or critical path) to determine the total tensile force in each critical region. The required steel area in each region was determined by dividing the total tensile force by the design strength of the steel (i.e., f_{sy}=60 ksi). Since this reinforcement was designed not to yield, a safety factor was incorporated into the procedure. The safety factors used in the design of the test specimen typically ranged between 1.4 and 1.8 (note that a larger safety

factor can be used in practice). This process was repeated for each edge of each perforation. A similar procedure was also followed to calculate the critical shear forces in the horizontal and vertical chord members around the perforations (see Figure 7c). Then, the required shear reinforcement areas were determined following ACI 318 guidelines.
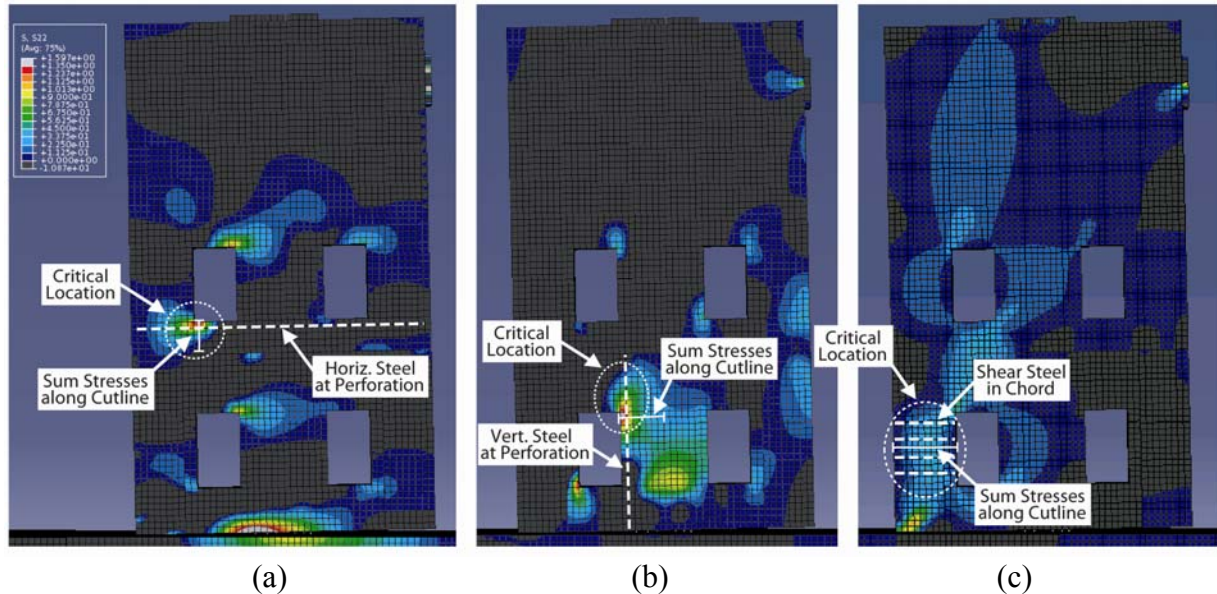

(a)   (b)   (c)

Fig. 7 Finite-Element Analytical Results: (a) *X*-Direction Tensile Stresses; (b) *Y*-Direction Tensile Stresses; (c) Shear Stresses

MEASURED BEHAVIOR

A reversed-cyclic lateral displacement history was used during the test, with three fully-repeated cycles at each displacement increment. The specimen sustained three cycles at a maximum drift of $\Delta_w=\pm3.05\%$ (which is above the ACI ITG-5.1 validation-level drift of $\Delta_w=\pm2.30\%$) prior to the indicating signs of failure due to the crushing of the confined concrete at the toes. The wall drift, Δ_w, was measured as the relative lateral displacement of the wall between the foundation and the lateral load location divided by the height to the lateral load. Figure 8a shows the wall at the end of the third cycle to $\Delta_w=+3.05\%$ and Figure 8b shows a close-up of the north base panel toe after the completion of the test.

While the perforations resulted in considerable shear deformations in the wall panels, the test specimen still behaved essentially as a rigid body, dominated by gap opening at the horizontal joint between the base panel and the foundation. The damage to the wall was concentrated in the base panel, with concrete cracking predominantly located in the horizontal chord members (both above and below the perforations) and in the center vertical chord (in between the perforations). The crack sizes generally remained small (the crack visible in the photographs in Figure 8 were highlighted with markers during the test for

enhanced viewing) indicating that the panel distributed reinforcement remained linear elastic as designed. Cover spalling and exposed confinement reinforcement was observed at both wall toes. Concrete cracking in the upper panel was limited to the corners of the perforations. No concrete crushing was observed in the upper panel and no significant gap opening was observed in the upper panel-to-panel joint. Shear-slip was insignificant across both the base joint and the upper joint.
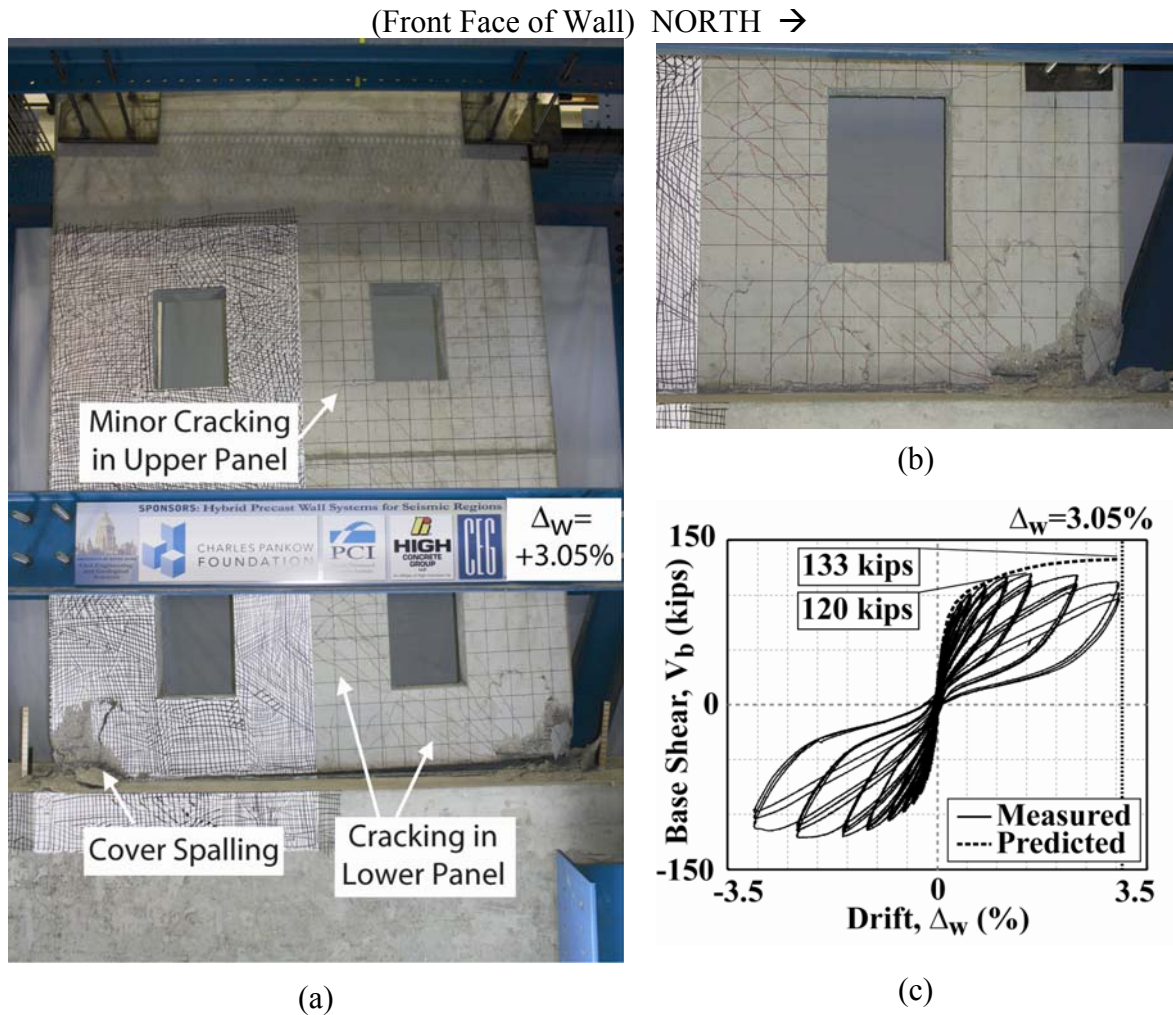
(Front Face of Wall) NORTH →

Fig. 8 Overall Behavior: (a) Specimen at Third Cycle to Δ_w=+3.05%; (b) North Wall Toe at Base Panel after Completion of Test; (c) V_b-Δ_w Response

Figure 8c shows a comparison of the measured base shear force, V_b, versus wall drift, Δ_w, behavior of the test specimen with the finite-element analytical model. The specimen demonstrated full re-centering capability while also providing large energy dissipation due to the combination of unbonded PT steel with yielding mild steel reinforcement across the base-panel-to-foundation joint. While crushing of the confined concrete was beginning to dominate at the wall toes, the total strength loss at the completion of the drift history (through

the cycles at $\Delta_w=\pm3.05\%$) was less than 20%, thus satisfying the ACI ITG-5.1 requirement for validation.

The analytical results provided a reasonable match for the measured behavior, especially considering the intentional simplifications incorporated into the model. Small discrepancies exist, particularly an overestimation of the base shear force at the validation-level and maximum drifts. This discrepancy is related to the inability of the simple concrete material models to properly capture the confinement effects and the degradation at the wall toes. While a more sophisticated finite-element model may better capture the concrete behavior, the reasonable correlation between the analytical and experimental load-displacement behaviors along with the relatively small damage to the wall after the completion of the test (i.e., distributed cracking at the base panel and cover concrete spalling at the wall toes) demonstrate that the existing model can be an effective design tool for engineers to use in practice.

SUMMARY AND CONCLUSIONS

This paper presents the results from a research project investigating the design and behavior of hybrid panelized precast concrete shear wall structures for seismic regions. The design, predicted behavior, and measured performance of a 0.4-scale wall test specimen featuring two rectangular perforations in each panel are discussed. A finite-element analytical model is presented and the results of a pre-test monotonic pushover analysis are used to design the horizontal and vertical bonded reinforcement around the panel perforations as well as the shear reinforcement in the panel chord members. The analytical study is compared with the measured results from the test specimen subjected to reversed-cyclic lateral loading. The wall behaved as designed, sustaining three cycles at the required validation-level drift ($\Delta_w=\pm2.30\%$) as well as three cycles at a greater drift of $\Delta_w=\pm3.05\%$. The observed damage was concentrated in the base panel, consisting of cracking in the horizontal chord members (both above and below the perforations), cracking in the center vertical chord, and concrete crushing at the wall toes. The analytical predictions displayed a reasonable match with the measured results, demonstrating that the finite-element model used to design the reinforcement around the perforations can be an effective tool for engineers in practice. Future experimental and analytical work featuring larger panel openings has been planned and will be used to further explore the modeling approach.

ACKNOWLEDGEMENTS

REFERENCES

1. ACI 318, "Building Code Requirements for Structural Concrete (ACI 318-08) and Commentary," *ACI Committee 318*, Farmington Hills, MI, 2008.

2. ACI ITG-5.1, "Acceptance Criteria for Special Unbonded Post-Tensioned Precast Structural Walls Based on Validation Testing and Commentary," *ACI Innovation Task Group 5*, Farmington Hills, MI, 2007.

3. ACI ITG-5.2, "Requirements for Design of a Special Unbonded Post-Tensioned Precast Shear Wall Satisfying ACI ITG-5.1 and Commentary," *ACI Innovation Task Group 5*, Farmington Hills, MI, 2009.

4. Smith, B., Kurama, Y., and McGinnis, M., "Design and Measured Behavior of a Hybrid Precast Concrete Wall Specimen for Seismic Regions," *Journal of Structural Engineering*, In-print (preprint article accessed from http://ascelibrary.aip.org/), 2011.

5. Rahman, A. and Restrepo, J., "Earthquake Resistant Precast Concrete Buildings: Seismic Performance of Cantilever Walls Prestressed Using Unbonded Tendons," *Univ. of Canterbury,* Research Report No. 2000-5, 2000.

6. Holden, T., Restrepo, J., and Mander J., "A Comparison of the Seismic Performance of Precast Wall Construction: Emulation and Hybrid Approaches," *Univ. of Canterbury,* Research Report No. 2001-4, 2001.

7. Kurama, Y., "Hybrid Post-Tensioned Precast Concrete Walls for Use in Seismic Regions," *PCI Journal*, V. 47, No. 5, 2002, pp. 36-59.

8. Kurama, Y., "Seismic Design of Partially Post-Tensioned Precast Concrete Walls," *PCI Journal*, V. 50, No. 4, 2005, pp. 100-125.

9. Allen, M. and Kurama, Y., "Design of Rectangular Openings in Precast Walls Under Combined Vertical and Lateral Loads," *PCI Journal*, V. 47, No. 2, 2002, pp. 58-83.

10. Mackertich, S., and Aswad, A., "Lateral Deformations of Preforated Shear Walls for Low and Mid-Rise Buildings," *PCI Journal*, V. 42, No. 1, 1997, pp. 30-41.

11. Smith, B. and Kurama, Y., "Design of Hybrid Precast Concrete Walls for Seismic Regions," *ASCE Structures Congress*, Austin, TX, 2009, 10 pp.

12. Hibbitt, Karlsson, and Sorenson, "ABAQUS User's Manual - Version 6.9," Hibbitt, Karlsson & Sorenson, Inc., 2009.

13. Popovics, S., "A Numerical Approach to the Complete Stress-Strain Curves for Concrete," *Cement and Concrete Research*, V. 3, No. 5, 1973, pp. 583-599.

14. Mander, J., Priestly, M., and Park, R., "Theoretical Stress-Strain Model for Confined Concrete," *ASCE Journal of Structural Engineering,* V. 114, No. 8, 1988, pp. 1804-1826.